Korean J. Chem. Eng., **19**(4), 711-717 (2002)

The Effect of Particle Shape on the Pressure Drop across the Dust Cake

Joo-Hong Choi†, Soon-Jong Ha and Young-Ok Park*

Dept. Chem. Eng./ERI, Gyeongsang National University, Chinju 660-701, Korea
*Korea Institute of Energy Research, Daejeon 305-343, Korea
(*Received 31 January 2002 • accepted 16 March 2002*)

Abstract−In order to observe the effect of particle shape of poly-dispersed dusts on filter performance, the pressure drop across the dust cakes of fly ashes from a conventional power plant (PC), fluidized bed combustion (FBC), and paint incinerator (FI) was measured over a metal filter element in the accurate conditions. A fluidized bed column was used to prepare the dust feed stream of uniform particle distribution. The fine particles of FI ash have a tendency to be agglomerated at low transport velocity. The aggregates were broken at high velocity of more than 21 cm/sec. FBC ash composed of jagged type particles and containing high concentration of unburned-carbon showed higher pressure drop than that of PC ash composed mostly of spherical particles. FI ash composed of aggregates of very fine carbon particles presented the highest pressure drop among the fly ashes tested. The shape factors of PC, FBC, and FI ash were estimated as 0.91, 0.76, and 0.65, respectively, by the Ergun equation. The results implied that the irregular particle tends to form a higher pressure drop and to be more compressible than spherical one.

Key words: Shape Effect, Pressure Drop, Metal Filter Element, Fly Ash, Gas, Filtration

INTRODUCTION

Filtration is one of the most advantageous methods for removing particles from every kind of gas/solid system since it provides very high collection efficiency and is applicable at high temperature and pressure in order to achieve a thermally efficient and economical system. This has led to a renewed interest in filtration. Recently, filtration systems have been applied to many advanced systems like gasification, fluidized combustion, incineration, and chemical processes [Choi, 1999; Mitchell, 1997; Park et al., 2000, 2001; Yoa et al., 2001].

For the continuous operation of the filter, the filter element should be cleaned periodically when the pressure drop of the system reaches a tolerable limit by reverse flow or by pulse cleaning. In the normal cleaning step, the dust cake of the transition layer is detached when the cleaning force overcomes the binding force of the dust cake. So pressure drop of the filtration system is a main factor for the normal operation and the design of the filter system. The root of the pressure drop across the dust cake is mainly the structure of the dust cake denominated by the cake porosity. In general, the porosity of a packing body is lower for the particles of larger size, of poly-dispersed than mono-dispersed dust, and of lower shape factor [Perry and Green, 1973]. Even for the spherical uniform particle, the porosity of the packing body has the value of 0.260 (rhombohedral)-0.476 (cubic) according to the array method. The compressibility due to the binding forces of the particles and the face velocity difference is also another factor affecting the porosity of the dust cake. So it is very complicated to estimate the pressure drop of the composite dust. Therefore, the filtration conditions should be adjusted with the system to system since the particle properties from different sources are quite different. The key factors affecting the filtration performance by particulate are pointed out by the dust loading, particle size distribution, shape factor, density, electric charge, chemical reactivity, and surface morphology [Cheung et al., 1998; Neiva et al., 1999]. Correlation about these factors is roughly expressed by Ergun equation for the general fabric filtration system using a fabric filter element [Aguiar and Coury, 1996]. However, data about the fly ashes from FBC and incinerator systems are rare.

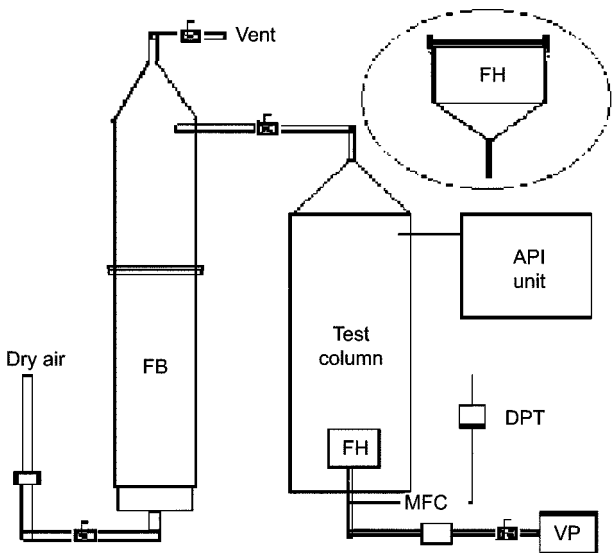

Fig. 1. The experimental unit for the measurement of pressure drop of filtration.
F/B: Fluidized bed
F/H: Filter holder
MFC: Mass flow controller
F/M: Flow meter
DPT: Differential pressure transmitter
VP: Vacuum pump

†To whom correspondence should be addressed.
E-mail: jhchoi@nongae.gsnu.ac.kr
‡This paper is dedicated to Professor Wha Young Lee on the occasion of his retirement from Seoul National University.

Primary focus of this study is to observe the pressure drop tendency of fly ashes of different particle shape. For the purpose of this work, fly ashes from conventional power plant (PC ash), fluidized bed combustion (FBC ash), and paint incinerator (FI ash) were chosen.

EXPERIMENTAL

Fig. 1 shows the schematic diagram of the experimental unit. The particle size of the fly ashes from PC ash (collected by the 3rd electric precipitator of a conventional power plant), FBC ash (collected by the 3rd electric precipitator of Donghae FBC power plant), and FI ash (collected by a ceramic filter unit in a waste paint incinerator) were classified in the fluidized column in order to get a uniform dust stream by using the dry air and directly fed to the test column. The proper amount of fly ash was filled initially and entrained at a given superficial velocity. The entrained stream of the fluidized bed was chosen for the experimental dust. A part of the dust stream was introduced into an in-situ aerodynamic particle size analyzer (API Aerosizer) from the top of the test column in order to measure the particle size distribution. In order to reduce the side effect from the pressure of the main stream, the outlet of the main stream was freely ventilated in a water bath. The face velocity across the filter element was exactly controlled with a mass flow controller connected to the vacuum pump. Pressure drop was measured by a differential pressure transducer and recorded in the time variance. The fresh filter element was used for each run. The metal filter element was fabricated with the metal fiber meshes and composed with three layers. Its average pore size is about 100 μm as shown at Fig. 2. The disk filter element of 6 cm diameter was fixed in the filter holder in the way that most of the particles introduced into the test column were collected on the filter element. The dust amount loaded during the filtration was weighed after a run. The dust was loaded linearly in the time variance during the first filtration of about 30 minutes.

RESULTS AND DISCUSSION

The samples of the fly ashes used in the experimental have different composition especially in the carbon content as shown in Table 1. FI ash contains the highest amount of carbon, about 52% with the high concentration of CaO and PbO. The composition of unburned carbon in FBC ash is about 23%. Table 2 shows the physical properties of the raw fly ashes from the plant site. The volume average mean particle sizes of raw fly ashes were analyzed with a mastersizer (Malvern instrument). Three kinds of fly ashes having an aerodynamic size of particles entrained at the superficial veloc-

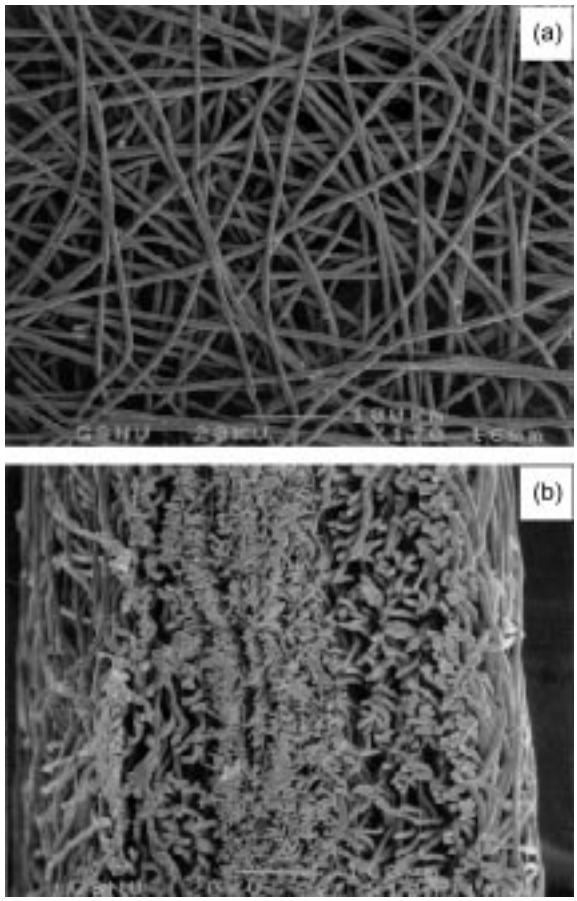

Fig. 2. SEM images of the fresh metal filter element for the normal (a) and thickness (b) plane.

Table 1. The chemical compositions of the raw fly ashes

Components (%)	SiO_2	Al_2O_3	Fe_2O_3	CaO	SO_3	K_2O	PbO	TiO_2	C
PC ash	49.0	29.4	6.0	5.4	0.9	-	-	1.6	5.6
FBC ash	33.4	26.7	3.1	5.9	2.1	-	-	1.6	23.0
FI ash	18.2	1.1	0.6	10.9	-	0.6	4.9	1.3	52.1

Table 2. Physical properties of the raw fly ashes

Property	Method	PC ash	FBC ash	FI ash
Volumetric mean particle size (μm)	Mastersizer	19.15	45.68	37.55
True density	Le Sattlier	2.381	1.825	1.026
Bulk density	-	0.772	0.545	0.164
Packing porosity (%)	-	67.6	70.1	80.0
Specific surface area (m^2/g)	Mastersizer	5.5	48.4	170.5
Morphology	SEM	Spherical	Jagged	Aggregated

Table 3. The geometric particle sizes of fly ashes classified in the fluidized bed

V_o, cm/s	PC ash, μm	FBC ash, μm	FI ash, μm
5	4.30	4.88	11.10
13	6.70	6.66	7.45
21	11.17	11.72	4.46

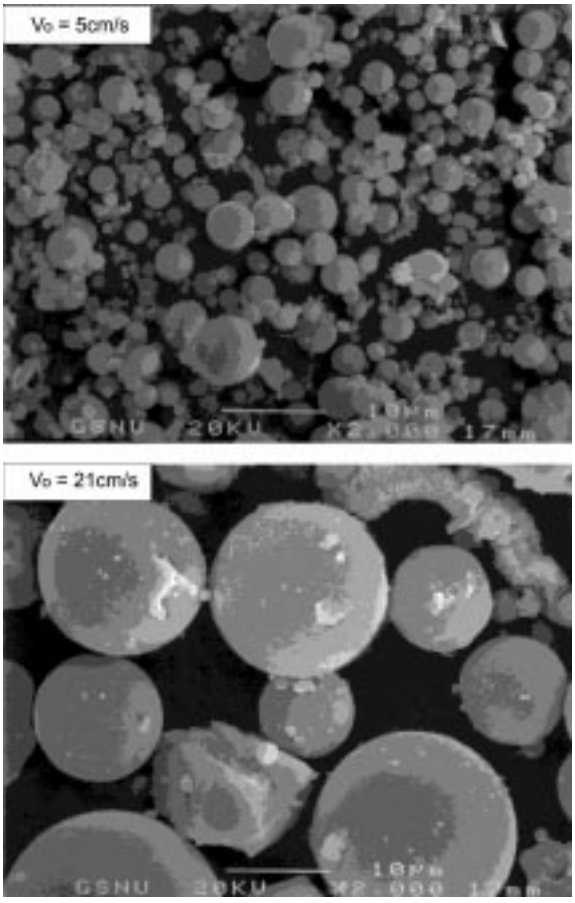

Fig. 3. SEM images of PC ash entrained at the given V_o.

ity (V_o) of 5, 13, and 21 cm/s were prepared in the fluidized bed column. Each sample prepared at the same superficial velocity is assumed to have the same aerodynamic particle size. However, the geometric mean particle sizes (d_g) are slightly different as shown in Table 3 since their densities are different. The particle size of FI ash at high superficial velocity (V_o) is reduced since the aggregates are broken due to the high attrition force at the high velocity. Sauter mean diameters of the fly ashes were slightly larger than those of the geometric mean particle sizes.

Fig. 3 shows SEM images of the PC ash collected in the filter element for the different superficial velocity. Most of the particles are spherical and similar to the fused-flue dust defined in literature [Perry and Green, 1973]. According to Perry and Green, the shape factor of this kind is 0.89. The largest particles are cut at the low superficial velocity. So the classified particles present a monomial mode of particle distribution compared to the binomial mode of the raw ash.

As shown in Fig. 5, FBC ash presents the jagged type that is similar with the crushed-class defined in the literature [Perry and Green, 1973]. They reported that the shape factor of this type is 0.65. FI ash showed quite different type of particles that are agglomerated at low superficial velocity of fluidized bed. The agglomerated particles are busted at high velocity as shown in Fig. 6 that presents the smaller particle size as the larger superficial velocity. It was observed that the original size of the agglomerated particle is less than 1 μm as shown in the last figure of Fig. 6. The agglomerated particles are more similar with the flue dust aggregates defined in the litera-

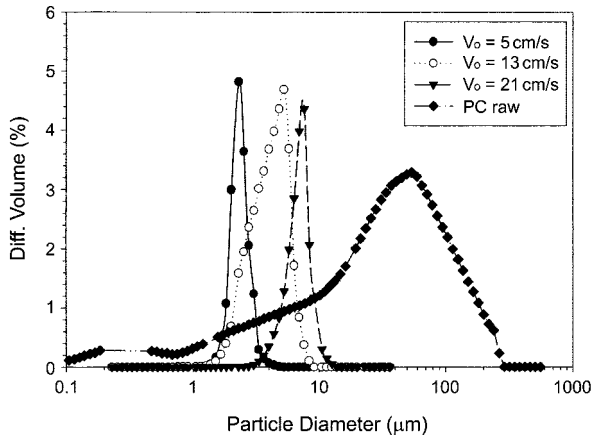

Fig. 4. The particle size distribution of the PC ash entrained at different V_o in the fluidized bed.

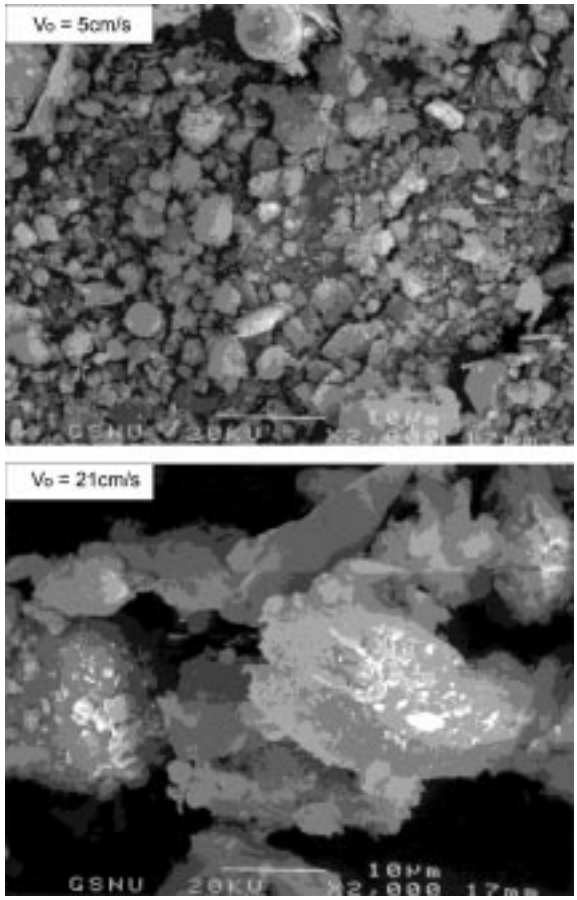

Fig. 5. SEM images of FBC ash entrained at the given V_o.

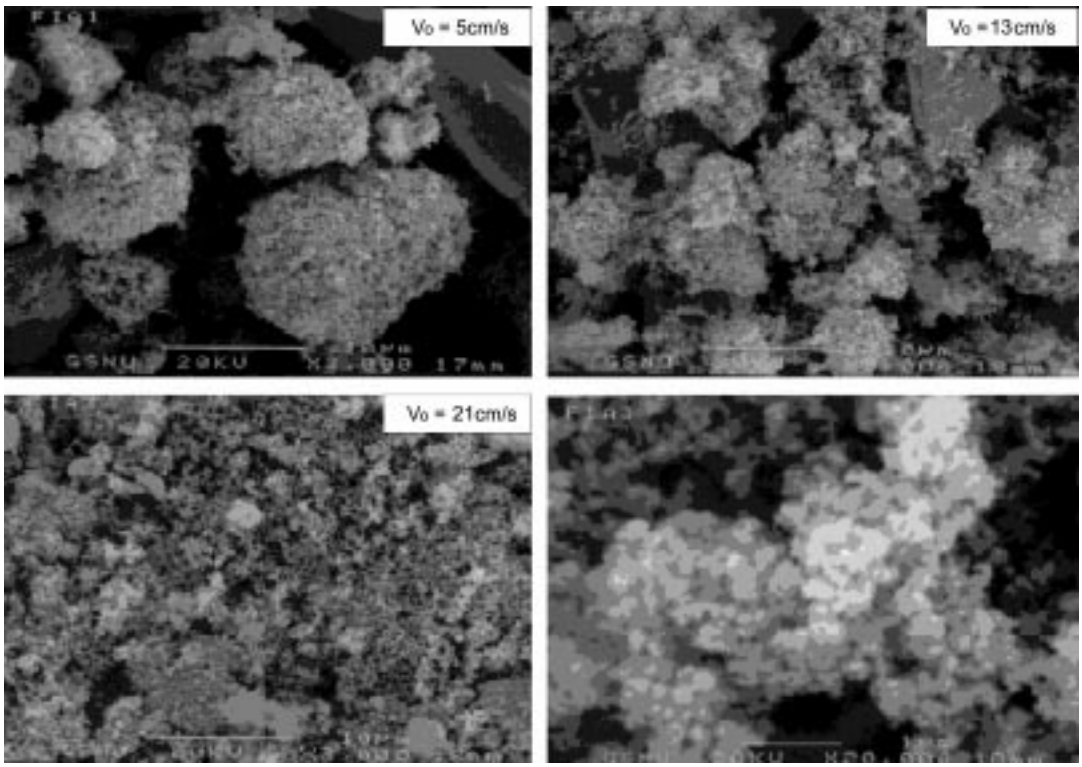

Fig. 6. SEM images of FI ash entrained at the given V_o.

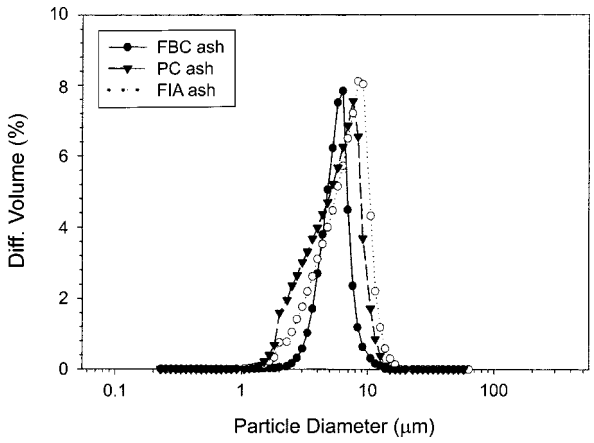

Fig. 7. The particle size distribution of fly ashes entrained at V_o= 13 cm/s.

ture [Perry and Green, 1973] having the shape factor of 0.55. Fig. 7 represents the typical pattern of the particle size distribution of the three samples for V_o=13 cm/s. FI and FBC ash is cut more clearly than PC ash. And their sizes are relatively larger than that of PC ash because their densities are low. Table 3 denotes the several mean particle sizes that classified by the superficial velocity of the fluidized bed.

The total pressure drop (ΔP_T) of the filtration denotes the sum of those across the filter element (ΔP_F) and the dust cake (ΔP_C) and expressed by Eq. (1) by using Darcys law. The filter drag (S) represents the value of the pressure drop over the face velocity like Eq. (2). It is linear with the value of the area dust load (W) at the narrow range of the real operation conditions [Cheung et al., 1998; Neiva et al., 1999]. The filter drag coefficient (K_2) of the equation is the key value in order to predict the property of the dust cake. And it is a function of the factors like porosity (ε), particle density (ρ_p), particle shape factor (φ_s), mass mean particle size (d_p), Sauter mean particle size (d_s), and gas viscosity (μ). And the filter drag coefficient (K_2) may be expressed by Eq. (3) [Neiva et al., 1999] or Eq. (4) [Aguiar and Courry, 1996] by using the Kozeny-Carman equation based on the Ergun equation [Ergun, 1952]. Eqs. (3) and (4) have been adopted usefully for poly-disperse particles even though they are semi-empirical for the mono-disperse dusts [Cheng and Tsai, 1998; Aguiar and Courry, 1996].

$$\Delta P_T = \Delta P_F + \Delta P_C = k_1 V_f + k_2 V_f W \tag{1}$$

$$S = \frac{\Delta P_C}{V_f} = K_2 W \tag{2}$$

$$K_2 = \frac{180(1-\varepsilon)}{\varepsilon^3} \cdot (\rho_P \varphi_S^2 d_p^2)^{-1} \cdot \mu \tag{3}$$

$$K_2 = \frac{150(1-\varepsilon)}{\varepsilon^3} \cdot (\rho_P d_s^2)^{-1} \cdot \mu \tag{4}$$

For the fly ashes used in the study, the particle density and the shape factor are higher in the order of PC ash>FBC ash>FI ash. Because the product of these two factors has also the same order, the estimated value of pressure drop by Eq. (3) increases in the order of FI ash>FBC ash>PC ash for the similar particle size. Fig. 8 shows the filter drag of FI ash is the highest, followed by FBC ash and PC ash in the order for the similar particle size entrained at V_o=13 cm/s. This result denotes that the shape factor is very dominant ele-

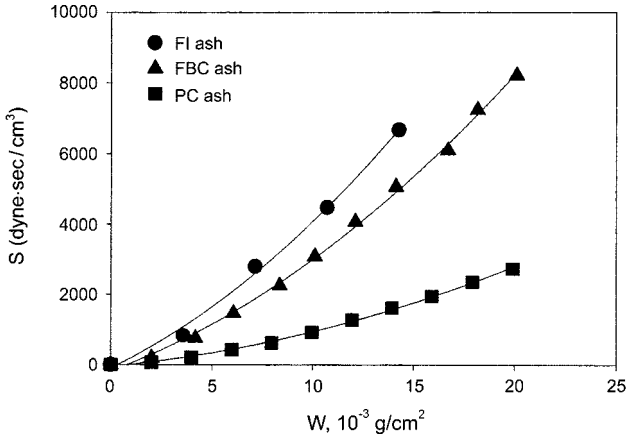

Fig. 8. The effect of particle type on the filter drag for V_o=13 cm/s and V_f=6 cm/s.

ment in determining the filter performance of the poly-disperse particles.

S-W curve for fly ashes over the metal filter element showed upward curvature at initial time of dust load and tend to approach the linear curve at high load after the filter element is conditioned. The conditioning time was long because the pores are continuously plugged with the penetrating particles through the deep bed of the filter. The high tendency of the upward curvature implies high compression of the dust layer or high penetration of the dust particles. The last effect is negligible in this study since the dust layer is too thin to be compressed at the initial stage of the filtration. In the case of PC ash, the variation of the filter drags with the particle size and the face velocity is relatively small as shown in Fig. 9 and Fig. 10, respectively. However, the filter drags for FBC ash and FI ash are noticeably higher as the particle size is smaller and the face velocity is higher as shown in Figs. 11-14.

Table 4 presents the K_2 values measured in the linear region of S-W curve measured at the face velocity of 6 cm/s for the fly ashes entrained at V_o=13 cm/s. The filter drag coefficients of FBC and FI ashes are higher than that of PC ash, which can be expected by Eq. (3), because the density and the shape factor are lower than those

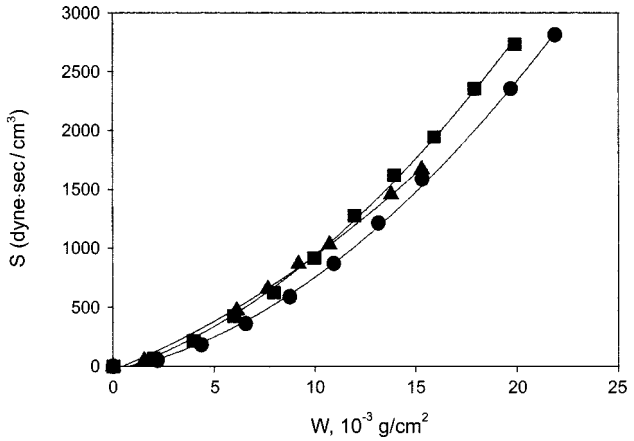

Fig. 9. The filter drag of PC ash at V_f=6 cm/s in the variance of dust load for the particle size of (■) 11.17, (▲) 6.70, and (●) 4.30 μm.

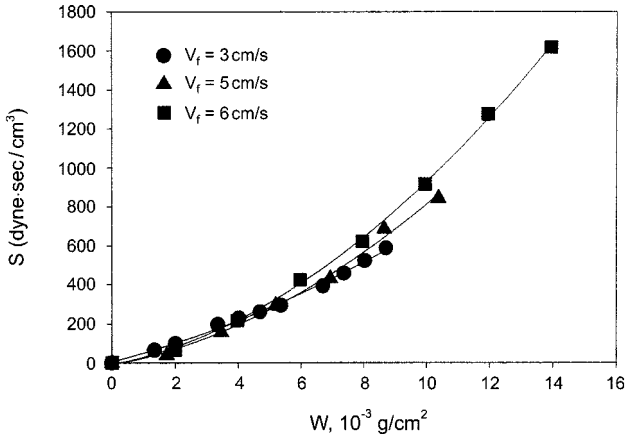

Fig. 10. The effect of face velocity on the filter drag of PC ash.

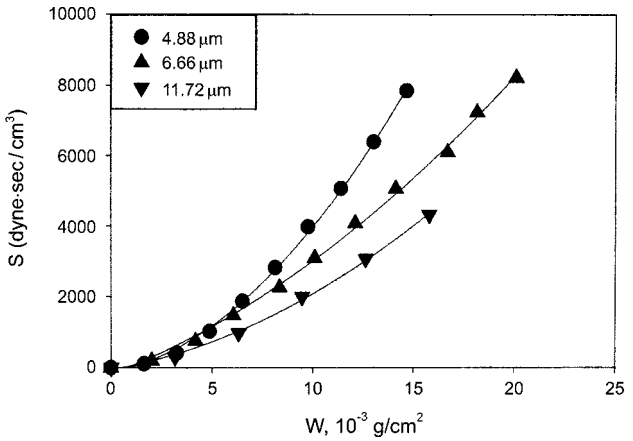

Fig. 11. The effect of particle size on the filter drag of FBC ash at V_f=6 cm/s.

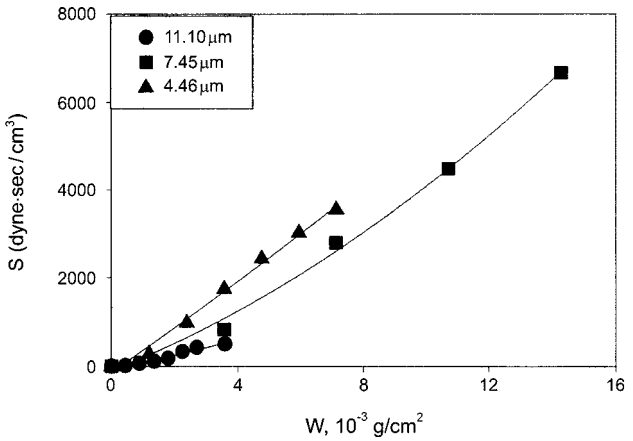

Fig. 12. The effect of particle size on the filter drag of FI ash at V_f=6 cm/s.

of PC ash, even though the particle size is larger. The porosities of the dust cake are shown in Table 4. The cake porosity of PC ash was higher than that of FBC and FI ashes, which implies that the shape factor is the dominant factor for the filter drag. As shown at Figs. 9-13, the filtration drag deviations with the particle size and the face velocity for FBC and FI ashes were larger than that of PC

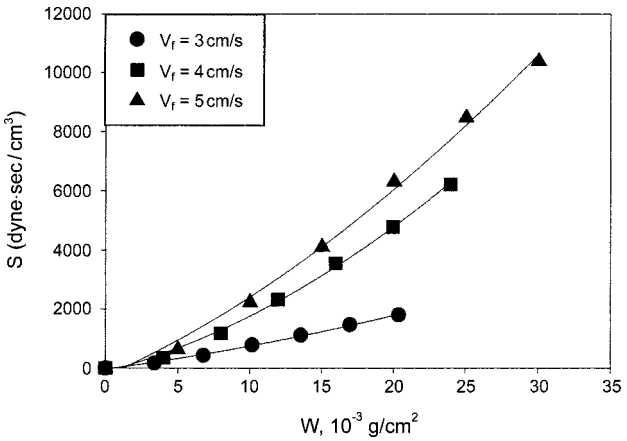

Fig. 13. The effect of face velocity on the filter drag of FBC ash entrained at V_o=21 cm/s.

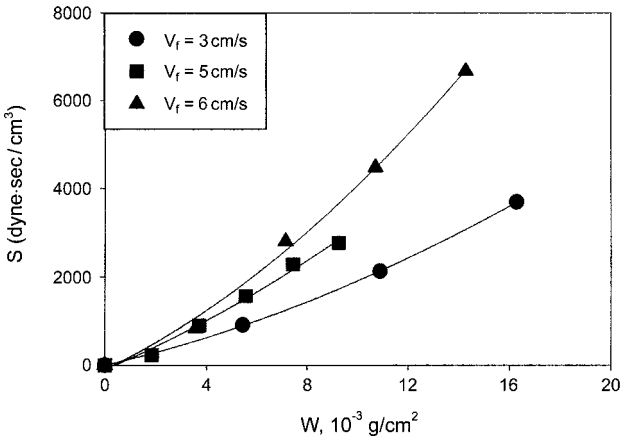

Fig. 14. The effect of face velocity on the filter drag of FI ash entrained at V_o=13 cm/s.

ash for the ashes entrained at the same V_o. The result implies that the dust cake of irregular particles tends to be more compressible than that of spherical one. The shape factors calculated by Eq. (3) from the experimental data are shown in the last column of Table 4. The values are similar but slightly larger than those reported by the literature [Perry and Green, 1973]. The reason why the shape factors measured are larger is that the dust samples prepared with the fluidized bed column are more uniform than those of raw fly ashes.

CONCLUSIONS

In order to observe the effect of particle shape on filter performance, the filter drag of fly ashes from a conventional power plant (PC), fluidized bed combustion (FBC), and paint incinerator (FI) were measured over a metal filter element. The particle sizes of the fly ashes were classified on the fluidized bed column to prepare the sample having the same aerodynamic particle size. FBC ash was composed of irregular particles and contained a high concentration of unburned carbon. So its shape factor and density are low. PC ash was mostly composed of spherical particles and presented lower filter drag even though its particle size was smaller. FI ash aggregated with very fine carbon particles showed the highest pressure drop among the tested fly ashes. The fine particles of FI ash have a tendency to be agglomerated at low flow velocity. The filtration drag deviations with the particle size and the face velocity for FBC and FI ashes were larger than that of PC ash even though the particle size was larger. The result implies that the irregular particle tends to be more compressible than the spherical one.

NOMENCLATURE

d_g : deometric mean particle size [cm]
d_p : mass mean particle size [cm]
d_s : sauter mean particle size [cm]
K_2 : filter drag coefficient [s^{-1}]
S : filter drag [dyne·s·cm^{-3}]
V_f : face velocity [cm·s^{-1}]
V_o : superficial velocity in fluidized bed [cm·s^{-1}]
W : area dust load on the filter element [g·cm^{-2}]
ΔP_C : pressure drop in dust layer [dyne·cm^{-2}]
ΔP_F : pressure drop in filter layer [dyne·cm^{-2}]
ΔP_T : total pressure drop [dyne·cm^{-2}]
ε : porosity [-]
μ : air viscosity [g·s^{-1}·cm^{-1}]
ρ : particle density [g·cm^{-3}]
φ_s : shape factor of particle [-]

ACKNOWLEDGEMENTS

The authors would like to thank the Korea Energy Management Corporation, Korea Institute for Energy Research, and Institute for Advanced Engineering for its financial support.

REFERENCES

Aguar, M. L. and Coury, J. R., "Cake Formation in Fabric Filtration of Gases," *Ind. Eng. Chem. Res.*, **35**, 3673 (1996).
Cheung, Y. H. and Tsai, C. J., "Factors Affecting Pressure Drop Through a Dust Cake During Filtration," *Aerosol Science and Technology*, **29**, 315 (1998).
Choi, J. H., "Investigation into the Pulse Cleaning of the Ceramic Filter Candle," *High Temperature Gas Cleaning*, **2**, 200 (1999).
Ergun, S., "Fluid Flow Through Packed Columns," *Chem. Eng. Prog.*, **48**(2), 89 (1952).

Table 4. The measurement values for the dust cake of V_o=13 cm/s and V_f=6 cm/s

Ash	D_g μm	ρ_p g/cm^3	D_p μm	D_s μm	$K_2 \times 10^{-4}$ s^{-1}	ε %	φ_s reported	φ_s measured
PC	6.70	2.50	9.074	7.54	1.750	67.9	0.89	0.91
FBC	6.66	2.01	12.19	8.50	4.833	54.7	0.65	0.76
FI	7.45	1.03	8.22	12.65	5.874	53.2	0.55	0.65

Koch, D., Cheung, W., Seville, J. P. K. and Clift, R., "Effects of Dust Properties on Gas Cleaning Using Rigid Ceramic Filters," *Filtration & Separation*, **July/August**, 337 (1992).

Mitchell, S. C., "Hot Gas Particulate Filtration," IEA Coal Research, London, UK (1997).

Neiva, A. C. B., Goldstein, Jr. L. and Calvo, P., "Modeling Cake Compressibility on Gas Filters," *High Temperature Gas Cleaning*, **2**, 83 (1999).

Park, O. K., Kim, S. D., Son, J. E., Rhee, Y. W. and Choi, W. S., "Demonstration of a KIER-Type CYBAGFILTER System at the Clinker Calcination Process," *Korean J. Chem. Eng*., **17**, 579 (2000).

Park, O. K., Park, H. S., Park, S. J., Kim, S. D., Choi, H. K. and Lim, J. H., "Development and Evaluation of Multilayer Air Filter Media," *Korean J. Chem. Eng*., **18**, 1020 (2001).

Perry, R. H. and Green, D. W., "Perry's Chemical Engineerings' H/B," 6th ed., McGraw-Hill, 20 (1973).

Yoa, S. J., Cho, Y. S., Choi, Y. S. and Baek, J. H., "Characteristics of Electrostatic Cyclone/Bag Filter with Inlet Types (Lab and Pilot Scale)," *Korean J. Chem. Eng*., **18**, 539 (2001).